Supporting information

Fe/Fe_3C nanoparticles encapsulated in ZIF-8 derived carbon nanotubes as a cathode oxygen reduction catalyst for microbial fuel cells

Xinyi Wang[a], Xinlu Lin[b], Jie Zhou[b], Yinhua Jiang[c], Yuqiao Wang*[a]

[a]Research Center for Nano Photoelectrochemistry and Devices, School of Chemistry and Chemical Engineering, Southeast University, Nanjing, Jiangsu 211189, China

[b]Advanced Solar Power (Hangzhou) Inc., 801 Lingyun Street, Hangzhou 310018, China

[c]School of Chemistry and Chemical Engineering, Jiangsu University, Zhenjiang 212013, China

*Corresponding authors: Yuqiao Wang (Email: yqwang@seu.edu.cn).

[#]These authors contributed equally to this work.

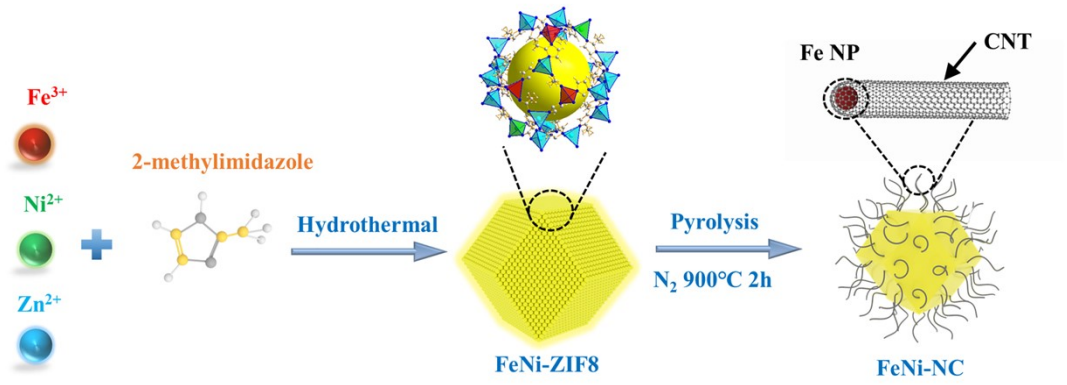

Figure. S1. Schematic illustration for synthesis of Fe/Fe_3C@NiNC.

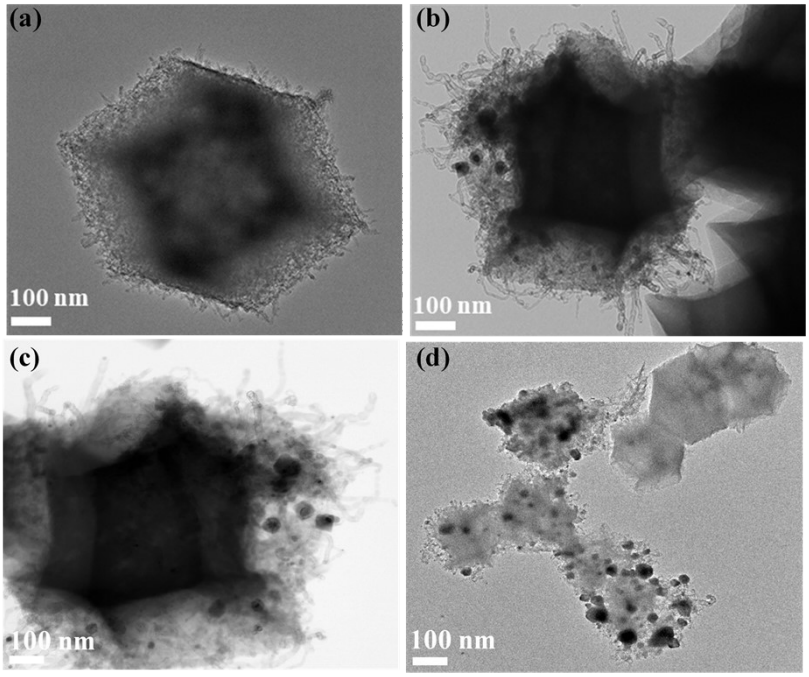

Figure. S2. TEM images of Fe/Fe_3C@NiNC.

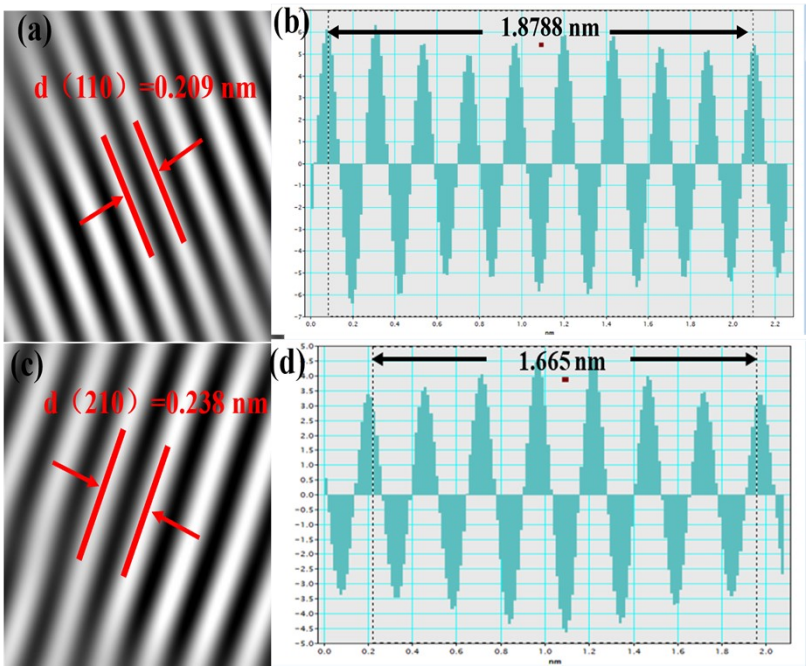

Figure S3. Enlarged HRTEM lattice fringe images of Fe/Fe_3C@NiNC. (a–b) Fe phase; (c–d) Fe_3C phase.

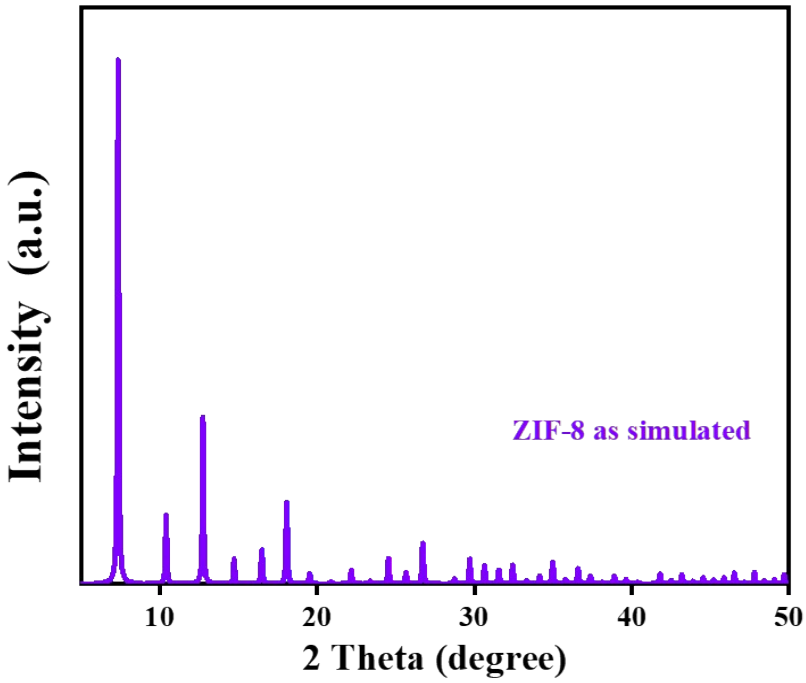

Figure. S4. XRD patterns of simulated ZIF-8 precursor.

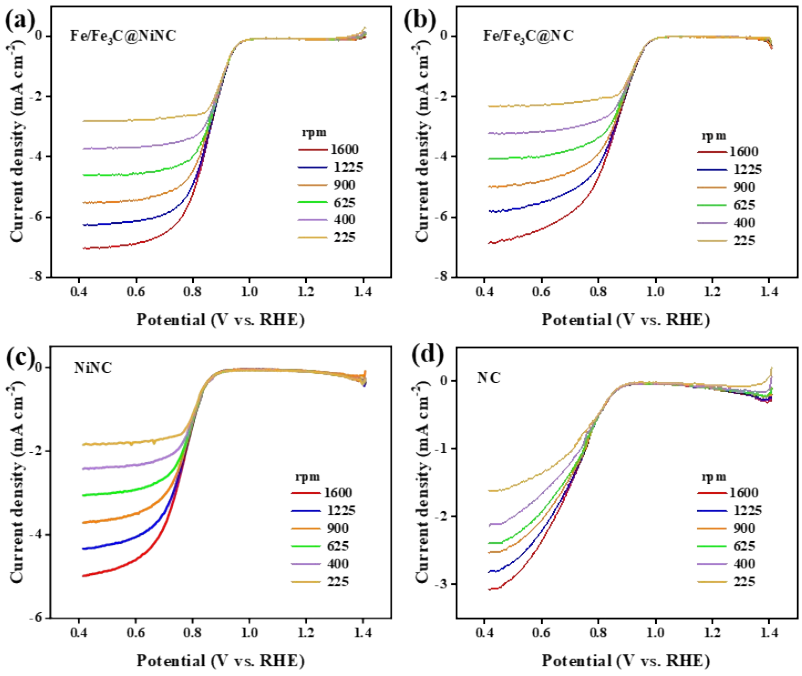

Figure. S5. LSV with different electrode rotation speeds of (a) Fe/Fe_3C@NiNC, (b) Fe/Fe_3C@NC, (c) NiNC, (d) NC.

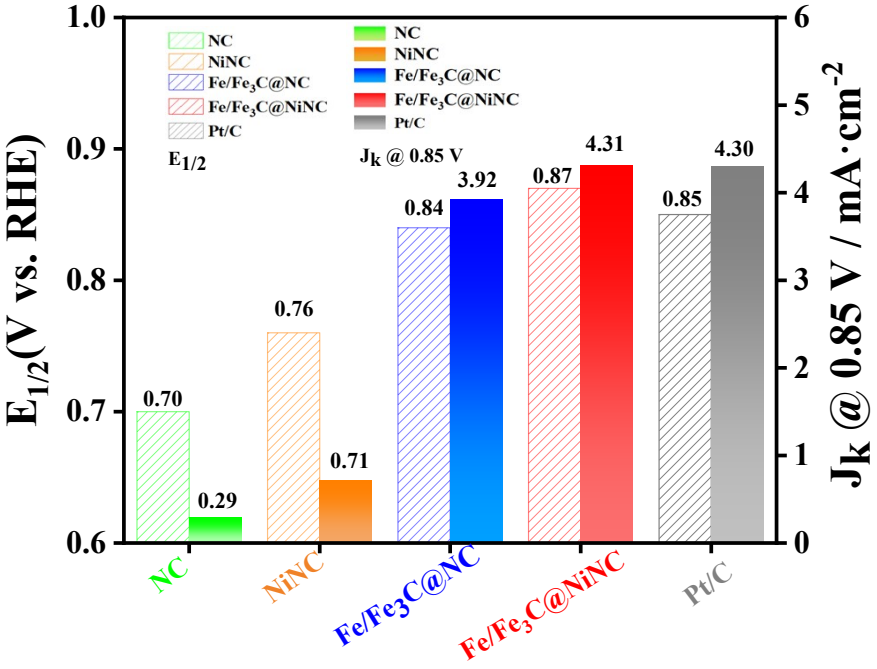

Figure. S6. Half-wave potential of $E_{1/2}$ and kinetic current density J_k.

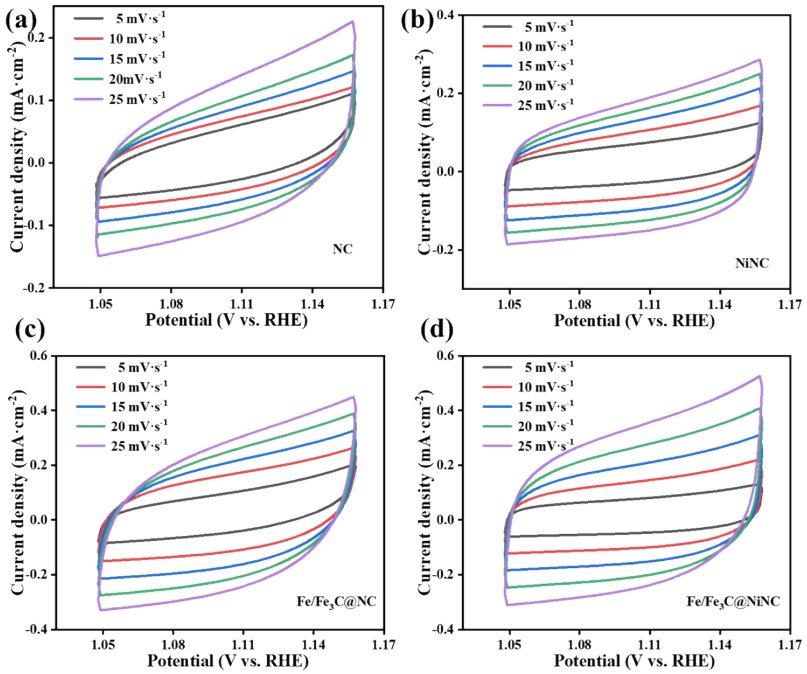

Figure. S7. CV curves of (a) NC, (b) NiNC, (c) Fe/Fe_3C@NC, (d) Fe/Fe_3C@NiNC at different scan rates (5, 10, 15, 20 and 25 mV s^{-1}).

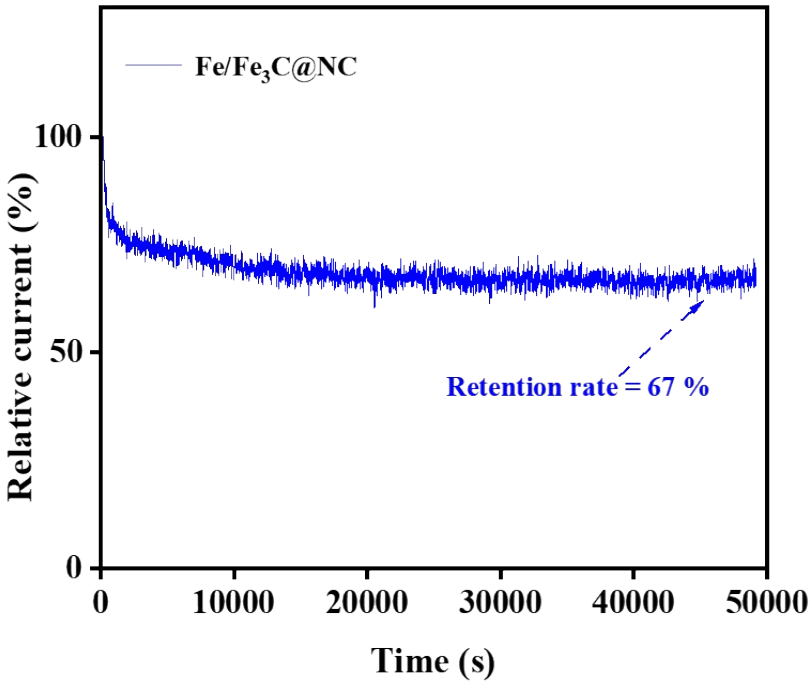

Figure. S8. Chronoamperometric response of $Fe/Fe_3C@NC$.

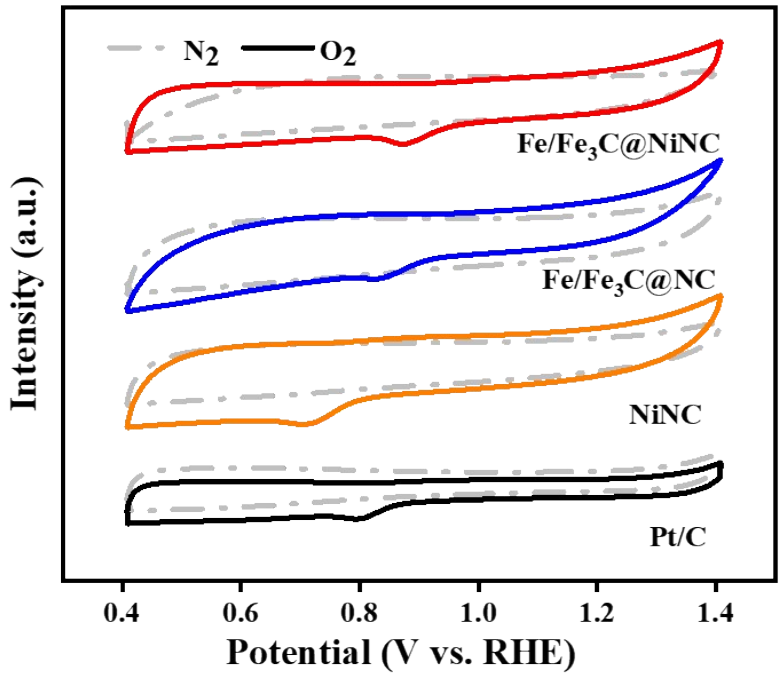

Figure. S9. CV curves in N_2-saturated 0.1 MKOH and O_2-saturated 0.1 MKOH of all catalysts.

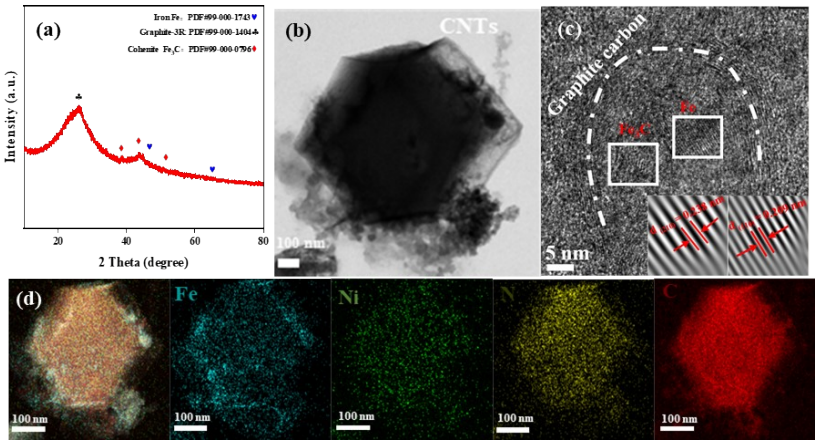

Figure. S10. (a) XRD image of Fe/Fe_3C@NiNC after ORR. (b and c) TEM images of Fe/Fe_3C@NiNC after ORR. (d) Elemental mapping images of Fe/Fe_3C@NiNC after ORR.

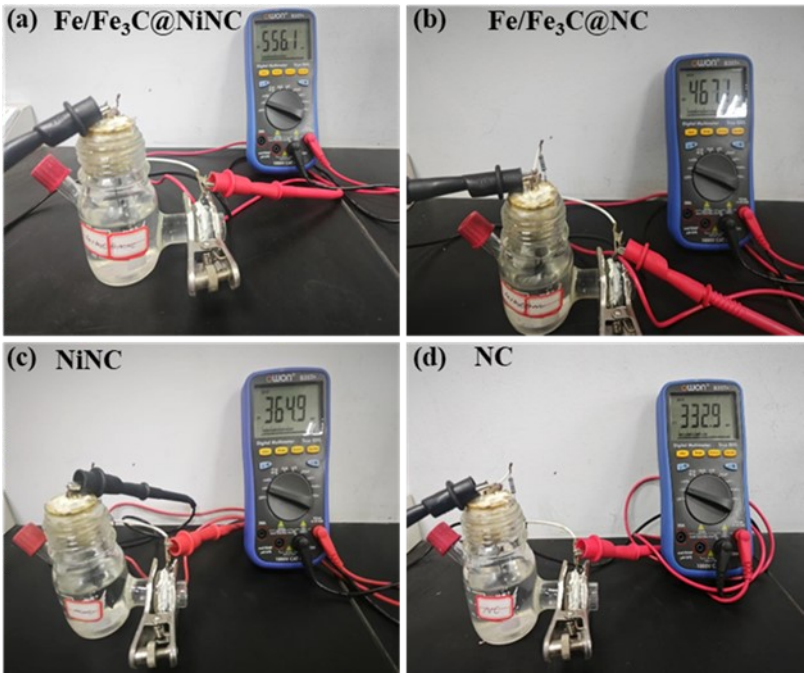

Figure. S11. The schematic diagrams of MFCs measurement.

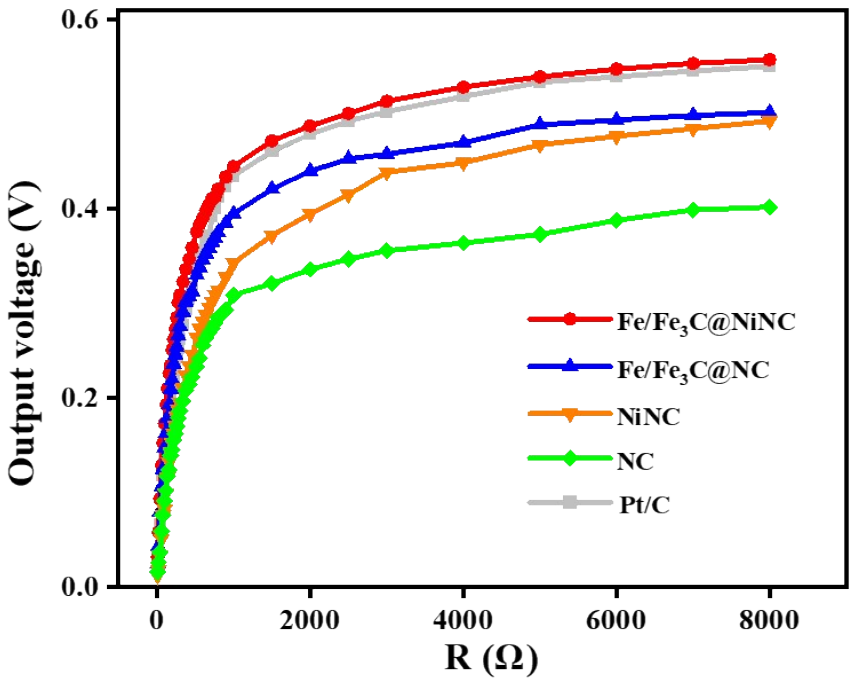

Figure. S12. The battery voltage under different external resistors.

Table S1. Actual mass ratio and atomic ratio of Fe/Fe_3C@NiNC obtained from XPS.

Elements	At%
C 1s	87.84
N 1s	10.51
Fe 2p	1.32
Ni 2p	0.33

Table S2. The content and distribution of different nitrogen species from N 1s XPS.

Catalysts	Pyri-N (%)	Pyrr-N (%)	Graph-N (%)	M-N (%)	Ox-N (%)
Fe/Fe_3C@NiNC	54.5	17.2	6.9	17.8	4.4
Fe/Fe_3C@NC	51.8	18.6	6.7	18.1	4.6
NiNC	50.8	20.8	7.1	17.2	3.5
NC	49.2	23.2	20.2	0	7.3

Table S3. The simulated data from EIS.

Catalysts	R_s (ohm cm^{-2})	R_{ct} (ohm cm^{-2})	R_w (ohm cm^{-2})
Fe/Fe_3C@NiNC	0.71	3.29	0.75
Fe/Fe_3C@NC	0.74	3.46	0.88
NiNC	0.77	4.28	1.87
NC	0.81	4.52	1.9

Table S4. Summary of ORR actives of various catalysts in 0.1 M KOH.

Catalysts	Half-wave Potential (V)	Onset Potential (V)	Limiting current density (mA cm^{-2})	Ref.
Fe/Fe_3C@NiNC	0.87	0.95	7.0	this work
Fe/S-N/C	0.84	0.95	5.9	[1]
FeMo-N-C	0.84	0.98	23.5	[2]
CoSn-NC	0.84	0.9	7.13	[3]
CoCu-LDH@NC	0.84	0.89	/	[4]
Co_4@Fe_1@NC	0.835	0.98	/	[5]
Fe_3C@NC	0.81	0.94	6.0	[6]
Cu_2O@Co/NC	0.8	0.89	3.8	[7]
CuCo@N/C	0.78	0.88	4.42	[8]

Table S5. The performance of air-cathode double-chamber MFCs equipped with the various ORR catalysts.

Anode	Cathode	External Resistance (Ω)	Output Voltage (mV)	Power Density ($mW \cdot m^{-2}$)	Ref.
Carbon cloth	Fe/Fe_3C@NiNC	1000	600	1600	this work
Carbon cloth	Ag@Co/Zn-NC	1000	470	1586	[9]
Carbon fiber brush	NPGC-1000	1000	650	1390	[10]
Carbon cloth	Cu/Co/N-HS	1000	620	1016	[11]
Carbon cloth	Cu/Co/N-C	1000	677	1008	[12]
Carbon felt	Fe_3C/Fe_2P@NC-N_4Fe_2	1000	597	949	[13]
Carbon cloth	Fe_4-N-C@TABOH	1000	670	830	[14]

Reference

[1]. Han W, Li C, Jiang Y, et al. Atomically-dispersed Fe-Nx and C–S–C ordered mesoporous carbons as efficient catalysts for the oxygen reduction reaction in a microbial fuel cell[J]. *Journal of Alloys and Compounds*, 2021, 852: 156994.

[2]. Zhu P, Xiong X, Wang X, et al. Regulating the FeN4 moiety by constructing Fe–Mo dual-metal atom sites for efficient electrochemical oxygen reduction[J]. *Nano Letters*, 2022, 22(23): 9507-9515.

[3]. Li L, Liu Z, Jiang D, et al. Bimetallic CoSn nanoparticles anchored on N-doped carbon as antibacterial oxygen reduction catalysts for microbial fuel cells[J]. *Nanoscale*, 2023, 15(38): 15739-15748.

[4]. Li L, Jiang D, Cai S, et al. N-Doped Carbon-Supported CoCu-Layered Double Hydroxide Nanosheets as Antibacterial Oxygen Reduction Catalysts for Microbial Fuel Cells[J]. *ACS Applied Energy Materials*, 2024, 7(7): 2854-2861.

[5]. Han A, Sun W, Wan X, et al. Construction of Co_4 atomic clusters to enable Fe–N4 motifs with highly active and durable oxygen reduction performance[J]. *Angewandte Chemie International Edition*, 2023, 62(30): e202303185.

[6]. Zhou Q, Yang Y, Ye Q, et al. Graphitic-nitrogen-enriched carbon skeleton with embedment of Fe_3C for superior performance air cathode in zinc-air battery[J]. *Materials Today Energy*, 2023, 31: 101194.

[7]. Chen H, Jiang D, Xie H, et al. Cu_2O@Co/N-doped carbon as antibacterial catalysts for oxygen reduction in microbial fuel cells[J]. *Environmental Science: Nano*, 2023, 10(1): 158-165.

[8]. Deng X, Imhanria S, Sun Y, et al. Mo, Fe bimetallic carbide composite as high stability electrocatalyst for oxygen reduction reaction[J]. *Journal of Environmental Chemical Engineering*, 2022, 10(3): 108052.

[9]. Jiang D, Chen H, Zhu L, et al. Ag@ Co/Zn N-Doped Carbon as Antibacterial Oxygen Reduction Catalysts for Microbial Fuel Cells[J]. *Energy Technology*, 2024: 2400062.

[10]. Wang W, Tang L, Chen C, et al. Engineering Pt–S–Mo and Pd–S–Mo sites in hierarchical porous MoS_2 for boosted oxygen reduction activity in microbial fuel cell[J]. *Journal of Power Sources*, 2024, 598: 234143.

[11]. Wang H, Wei L, Liu J, et al. Hollow N-doped bimetal carbon spheres with superior ORR catalytic performance for microbial fuel cells[J]. J*ournal of colloid and interface science*, 2020, 575: 177-182

[12]. Wang H, Wei L, Liu J, et al. Hollow bimetal ZIFs derived Cu/Co/N co-coordinated ORR electrocatalyst for microbial fuel cells[J]. *International Journal of Hydrogen Energy,* 2020, 45(7): 4481-4489.

[13]. Chu C, Liu J, Wei L, et al. Iron carbide and iron phosphide embedded N-doped porous carbon derived from biomass as oxygen reduction reaction catalyst for microbial fuel cell[J]. *International Journal of Hydrogen Energy*, 2023, 48(11): 4492-4502.

[14]. Jiang B, Jiang N, Cui Y, et al. Rapid Synthesis and Microenvironment Optimization of Hierarchical Porous Fe-N-C Catalysts for Enhanced ORR in Microbial Fuel Cells[J]. *Advanced Science*, 2024: 2402610.